Optica Applicata, Vol. XLI, No. 4, 2011

Investigation of optical detection strategies for transabdominal fetal heart rate detection using three-layered tissue model and Monte Carlo simulation

K.B. GAN[1*], E. ZAHEDI[2], M.A. MOHD ALI[1, 3]

[1]Institute of Space Science (ANGKASA), Universiti Kebangsaan Malaysia, 43600 Bangi, Selangor Darul Ehsan, Malaysia

[2]School of Electrical Engineering, Sharif University of Technology, Tehran, Iran

[3]Department of Electrical, Electronic and System Engineering, Faculty of Engineering, Universiti Kebangsaan Malaysia, 43600 Bangi, Selangor Darul Ehsan, Malaysia

[*]Corresponding author: gankokbeng@ukm.my

In this paper, the Monte Carlo technique is used to determine the optical detection strategies in three-layered (maternal, amniotic fluid and fetal) tissue model. This model is utilized to estimate the transabdominal optical power and optimum source–detector (S–D) separation. Results based on the launching of 2 million photons with 1 mW optical power showed that the expected optical power output is in the range of 10^{-6}–10^{-10} W/cm^2 depending on S–D separation. Considering the limit of the signal processing methods (such as adaptive noise cancelling) and the use of silicon photodetector, an S–D separation of 4 cm has been selected as a practical compromise between signal level and percentage of optical power (70%) coming from the fetal layer. Based on these findings, transabdominal fetal heart rate detection system using NIR and adaptive filtering can be designed and developed.

Keywords: transabdominal, fetal heart rate, Monte Carlo simulation, tissue model.

1. Introduction

Optical technique has received a considerable attention in biomedical diagnostics and monitoring of biological tissues such as brain imaging, breast imaging, and for fetal heart rate detection and oxygen saturation measurement due to its theoretical advantages in comparison with other modalities [1, 2]. Near infrared (NIR) light ranging between 650–950 nm [3] is only moderately absorbed by water, haemoglobin and other body substances, therefore can penetrate the human tissues and propagate

while in the tissue. The behaviour of the photon migration process in turbid media is a fundamental research in many practical applications in biological tissue. Monte Carlo algorithms of light propagation through turbid media have been utilized extensively in biomedical optics. They have been used to solve the radiative transport equation within the turbid medium as the analytical solution to the fact of its being complicated.

NIR spectroscopy has been applied to detect fetal oxygen saturation non-invasively via mother abdominal [4–9]. NIR light is non-ionizing and the power levels used are harmless to the body and therefore this technology is safe for continuous exposure. Moreover, NIR technology can be designed to be fast and portable and suitable in a clinical setting. In 2000, continuous wave NIR spectroscopy has been applied to non-invasive transabdominal fetal pulse oximetry. Transabdominal NIR spectroscopy was first proposed by RAMANUJAM *et al*. [4, 7–9], who used four 20 watt halogen lamps (10 cm separation from the pair of silicon photodetectors) and two 0.575-watt tungsten lamps (4 or 2.5 cm separation on either side of the pair of silicon photodetectors) as light sources and a pair of photodiodes as detectors. The cooling fans were used to reduce the heat generated by the halogen lamps. The measurements were made using NIR instrument from the maternal abdomen and tissue phantoms to investigate the photon migration process through fetal head. The photons are expected to migrate through both fetal and maternal tissues at large detector separation (7 cm) and reduced the error in the measurement caused by shunting [9]. Previous studies [4–9] show that the source–detector (S–D) separations depend on the type of source and the photodetector used in their studies. However, the above mentioned techniques use high power halogen lamps (a total of 80 W optical power provided by halogen lamps), laser diode and expensive photodetector (photomultiplier) to achieve desired signal-to-noise (SNR) ratio. These approaches are difficult to implement, especially in bedside or portable instruments for fetal heart rate (FHR) or oxygen saturation measurement in the future.

To overcome this problem, ZAHEDI and BENG [10] have proposed a low optical power technique using infrared and adaptive filtering. In [10], the maternal and fetal blood pulsations were emulated with typical SNR of –25 dB using a three-layered tissue model. The incoming light is modulated by the maternal and fetal blood pulsation, and as a result, the detected signal contains a mixture of maternal and fetal signal. The results showed that the adaptive noise cancelling using recursive least square algorithm is capable of extracting fetal signal up to –34 dB [10].

In [11], a low-power low-cost optical technique based on the photoplethysmogram (PPG) has been proposed for fetal heart rate detection using infrared and silicon detector. The proposed instrument utilizes low optical power, therefore appropriate S–D separation has to be justified for this specific application. The ability of digital signal processing technique to extract the fetal signal has to be in line with the practical implementation. By changing the type of source and detector, the S–D separation has to be altered so that the desired signal quality is achieved. The objective of this paper is to investigate the optical detection strategies for transabdominal fetal heart

rate detection. This paper discussed the selection of the optical components and S–D separation determination based on the Monte Carlo method for transabdominal FHR detection and oxygen saturation in the future.

2. Material and methods

2.1. Monte Carlo technique and ray tracing software

Monte Carlo simulation is a computational method for calculating the movement of photons within a tissue by launching millions of photons, and enables one to map the fluence rate distribution of photons. It is a flexible and accurate approach to simulate photon transport in tissues and produce multiple physical quantities. Monte Carlo technique has been utilized to estimate optical properties of tissues, which may be used to differentiate cancerous tissues from normal tissues [3, 12]. Besides, the light dosage for photodynamic therapy may be simulated using Monte Carlo method.

An excellent work has been done by WANG *et al*. [12] for Monte Carlo modelling of photon transport in multi-layered tissues. In this section, a brief discussion of the Monte Carlo simulation is given for the benefit of the readers. Instead of the numerical method, Monte Carlo approach solves the radiation transport problems [12] in a more realistic way. This technique divides the light source into many photon packets and interacts with the tissue model like energy particles of light which are scattered and absorbed. As photon interact with tissue, it will deposit weight due to absorption and the remaining weight will be scattered to other parts of the medium. Each photon packet will repeatedly undergo a number of steps until it is either terminated, reflected or transmitted. The optical properties that influence the light--tissue interaction are the absorption coefficient μ_a, scattering coefficient μ_s, anisotropy parameter g and refractive index n of the media. The launched photons depend on the desired SNR in the simulated measurement.

There is commercial software, namely TracePro and ASAP (The Advanced Systems Analysis Program), that can be used to perform the Monte Carlo simulation of the layered model. WANG *et al*. [12] had written a program in ANSI C for Monte Carlo modelling of photon transport in multi-layered tissues. The simulation software used in this work (TracePro version 3.0.0, Lambda Research Corporation) is a ray-tracing program for illumination, optical, radiometry, and photometry analysis. This software combines solid modelling, optical analysis features, strong data exchange capabilities, and is user friendly [13].

2.2. LED and detector model

There are various sources in the market used in diffuse optical measurement such as tungsten lamp with NIR filter, LED and laser diode. The purpose of the project is to develop a low power technique for FHR detection. LED is more suitable in this work as it provides the required spectrum (890 nm) and is inexpensive. An IR LED

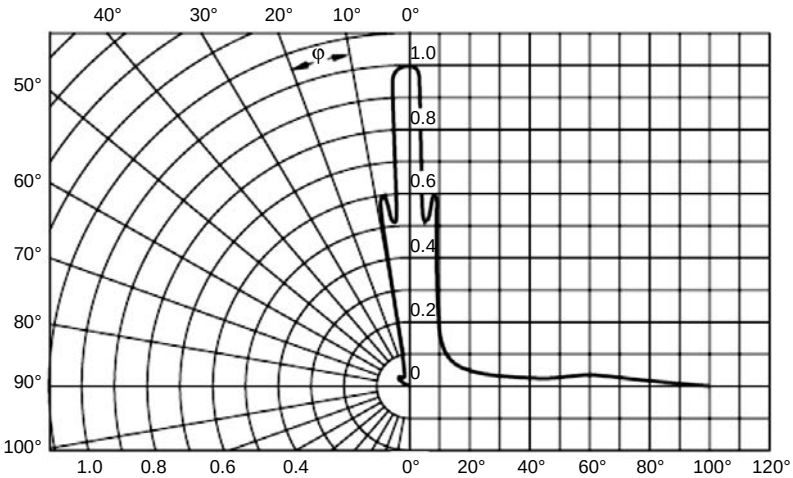

Fig. 1. Radiation pattern of selected LED (SFH-484-2, OSRAM Opto Semiconductors, Inc.)

(maximum power of 68 mW [11]) with the wavelength closest to the detector peak responsivity (900 nm) provided optimal penetration by placing the light source in contact with the skin and such that the beam is perpendicular to it. The measurement at 900 nm is affected by haemoglobin that is more transparent to infrared than oxyhaemoglobin [3].

In this study, the IR LED (SFH-484-2, OSRAM Opto Semiconductors, Inc.) is modelled. The proposed IR LED has wavelength closest to the low noise photodetector, where the peak responsivity occurred at 900 nm. The optical characteristic of the LED is given in Fig. 1. The detector model is an object where the surface property is a perfect absorber. Any incident light is absorbed and produces the output signal.

2.3. Photodetector

When designing an optical instrument, the detector is an essential component. Selection of an appropriate detector resulted in better signal quality of the acquired signals. The noise of the photodetector determines the maximum S–D separation which is useful in the optical instruments. Several types of detectors are recommended for diffuse optical measurements such as photomultiplier tubes, avalanche photodetector and silicon photodetector, and charge-coupled devices. The silicon photodetector is chosen in the optical FHR system as it is low cost compared to the photomultiplier tube. Furthermore, it can be placed directly onto the maternal abdomen without using any optical coupling cable like fiber optic one.

Currently, the low noise photodetector can be obtained from Edmond Optics Corporation with noise equivalent power as low as 1.8×10^{-14} W/Hz$^{1/2}$ (0.051 cm^2) (W57-522, Edmund Optics, Inc.) and 8.6×10^{-14} W/Hz$^{1/2}$ (1.00 cm^2) (W57-513, Edmund Optics, Inc.) Noise equivalent power is the incident optical power required to produce a signal on the detector that is equal to the noise when the SNR is equal to

T a b l e 1. Photodetector's noise (I_{PN}) during photovoltaic operation at various bandwidths where R is the responsivity and Rsh is the shunt resistance of the photodetector.

Photodetector area [cm^2]	R [A/W]	Rsh [MΩ]	Bandwidth [Hz]	I_{PN} [A]
0.051	0.62	600	100	8.29×10^{-14}
			1000	2.63×10^{-13}
			10000	8.29×10^{-13}
			100000	2.63×10^{-12}
1.00	0.62	30	100	3.71×10^{-13}
			1000	1.17×10^{-12}
			10000	3.71×10^{-12}
			100000	1.17×10^{-11}

one. A detector with 100 mm^2 active area, high responsivity at 900 nm (0.62 A/W) and low noise (8.6×10^{-14} W/Hz$^{1/2}$) from Edmund Optics, Inc., was selected in this study because the diffused reflected signal is very weak (10^{-6}–10^{-10} W/cm^2) at large S–D separation (4 cm). Compared to the PMT, the cost of silicon photodetector (USD 200) is about 10 percent of the PMT cost (USD 2000).

The photodetector can either operate in photovoltaic or photoconductance conditions. Photovoltaic operation offered a low noise system compared to the photoconductance operation. Shot noise (due to the dark current) is the dominant noise component during photoconductance operation. Small photodetector's active area results in lower noise level compared to the large photodetector's active area. Since the strong scattering process for the human tissue makes the light disperse in random fashion [14], large photodetector's active area increases the probability of detecting a photon that exit from the maternal layer. Therefore, a photodetector with 1 cm^2 area is proposed for the optical fetal heart rate instrument. This value has thus been used in the rest of this work. Table 1 shows the proposed silicon photodetector's noise I_{PN} during photovoltaic operation at various bandwidths. It can be seen that photodetector's noise increases with its bandwidth.

2.4. Three-layered tissue model

The anatomical model [15] shows the female abdominal area which includes components simulating the layers of tissue in this area, the female reproductive organs and the bladder. Previous work has outlined the use of the perturbation method in model photon transport through an 8 cm diameter fetal brain located at a constant 2.5 cm below a curved maternal abdominal surface with an air/tissue boundary [16]. In order to study the photo-migration process, the anatomical model has been simplified into a three-layered tissue model which has been reported in the literature [4, 9, 10]. In [10], a three-layered tissue model which consists of maternal, amniotic fluid and fetal layers has been proposed (Fig. 2). Maternal layer thickness d_M and amniotic fluid layer thickness d_{am} in this model are obtained from the literature.

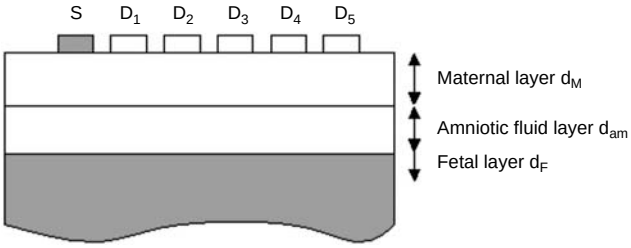

Fig. 2. A three-layered tissue model for light transport (not to scale) consisting of maternal, amniotic fluid and fetal layer. (S – source and D – detectors.)

In this work, the fetal layer thickness d_F is given infinite thickness so that it is close to the real-life conditions. As a result, light impinged on the fetal tissue will penetrate and travel into an unknown depth. Therefore, a finite fetal layer thickness which is given in [4] is not an appropriate boundary condition to perform the simulation. In order to obtain the optical power at various S–D separation, detectors D_1, D_2, D_3, D_4 and D_5 are placed at 2 cm, 4 cm, 6 cm, 8 cm and 10 cm, respectively, from the source S (Fig. 2).

Table 2 shows the optical properties (absorption, scattering and refraction index) of the tissue model which are obtained from the previous study. The aim of this simulation is to estimate the optical power at the photodetector using a three-layered tissue model. To calculate the percentage of light at the fetal layer, two different simulation conditions were provided, as listed below;

i) The maternal and amniotic fluid layers have optical properties as shown in Tab. 2. The fetal layer is given with infinitely high absorption.

T a b l e 2. Optical property of the proposed tissue model.

	Description	Symbol	Values	Units	References
Mother layer (M)	Absorption coefficient	μ_a(M)	0.08	cm^{-1}	[4]
	Reduced scattering	μ_s'	5	cm^{-1}	[4]
	Anisotropy	g	0.8	NA	[17]
	Refractive indices	n_r	1.3	NA	[19]
	Average maternal layer's pathlength	d_M	2.4±0.8	cm	[18]
Amniotic fluid layer (am)	Absorption coefficient	μ_a(am)	0.02	cm^{-1}	[4]
	Reduced scattering	μ_s'	0.1	cm^{-1}	[4]
	Anisotropy	g	0.85	NA	[4]
	Refractive indices,	n_r	1.3	NA	[19]
	Average amniotic fluid layer's pathlength	d_{am}	1.3±0.4	cm	[18]
Fetal layer (F)	Absorption coefficient	μ_a(F)	0.125	cm^{-1}	[4]
	Reduced scattering	μ_s'	5	cm^{-1}	[4]
	Anisotropy	g	0.8	NA	[17]
	Refractive indices	n_r	1.3	NA	[19]
	Average fetal layer's pathlength	d_F	∞	cm	[4]

ii) The maternal, amniotic fluid and fetal layers have optical properties as shown in Tab. 2.

The first simulation *i*) condition is used to obtain the maternal and amniotic fluid signal (P_{M+am}). All photons that reached the fetal layer are absorbed. The second simulation *ii*) condition is used to obtain the maternal, amniotic fluid and fetal signal (P_{M+am+F}). By subtracting P_{M+am} from P_{M+am+F}, fetal signal P_F is obtained.

Simulations have been performed at 2.5, 3.7 and 4.9 cm fetal depths, respectively, to calculate the expected optical power at the photodetector. Fetal depth is defined as the total thickness of the maternal and the amniotic fluid layer. The number of photons that have been injected into the maternal abdomen is obtained by trial and error. Two million photons with 3.5 mW/cm^2 (1 mW) optical power were selected to run the simulation. It takes approximately 9 hours to complete one simulation in Pentium IV 2.8 GHz processor.

3. Results and discussion

3.1. LED simulation

The polar candela distribution plot (radiation pattern) produced by the LED model in TracePro is shown in Fig. 3. Compared with Fig. 1, it can be seen that the simulated IR LED has the optical characteristic close to the actual LED.

3.2. Expected optical power and source–detector separation

The Monte Carlo simulation model is shown in Fig. 4. The simulation results show that the detection is made possible at 2.5 cm fetal depth even at the large S–D separation. When the fetal depth is increased to 3.7 cm and 4.9 cm, no signal is detected after 6 cm S–D separation. At this fetal depth, the losses are so high up to the moment the light reaches the fetal layer that they could not be detected by the detector.

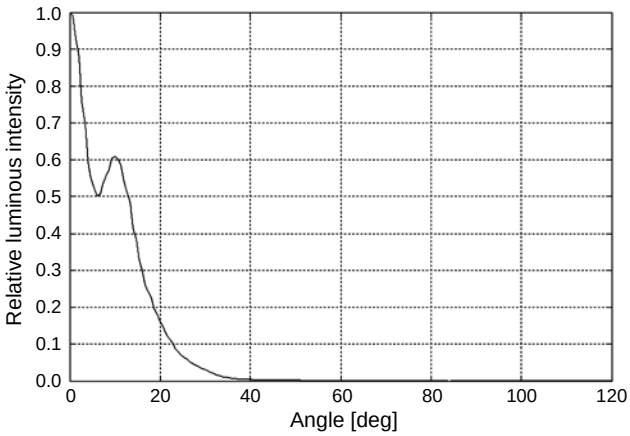

Fig. 3. LED simulation: polar candela distribution.

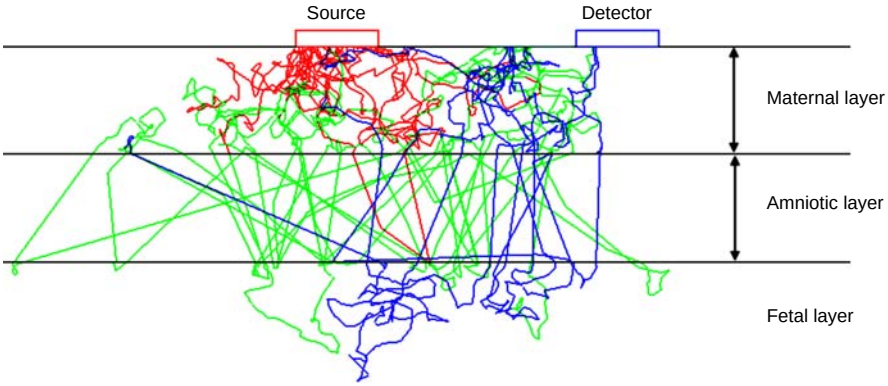

Fig. 4. Monte Carlo simulation model where red, green and blue colors indicate traces with high, moderate and low optical power, respectively, at 890 nm.

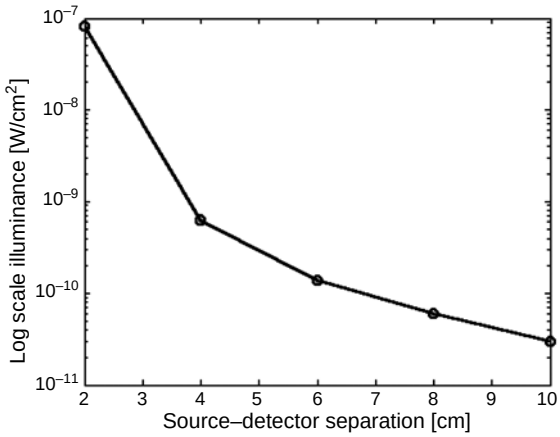

Fig. 5. Illuminance and the source–detector separation at 2.5 cm fetal depth.

This may be a first limitation of this technique and therefore the analysis is based on the 2.5 cm fetal depth simulation results.

The simulation results showed that the detected optical power by the photodetector is within 10^{-6}–10^{-10} W/cm^2 depending on the S–D separation (Fig. 5). The emitted optical power in this study is 1 mW and the fetal depth is 2.5 cm. From Figure 6, one can see that the optical power from the fetal layer increases with increased S–D separation. The simulation results showed that only 3% of the detected optical power comes from fetal tissue layer at 2 cm S–D separation. This value increases to 97% at 6 cm S–D separation.

3.3. Adaptive noise cancelling and photodetector limit

Since the adaptive noise cancelling limit is –34.7 dB, the photodetector used in the optical fetal heart rate instrument with 4 cm S–D separation must be able to detect

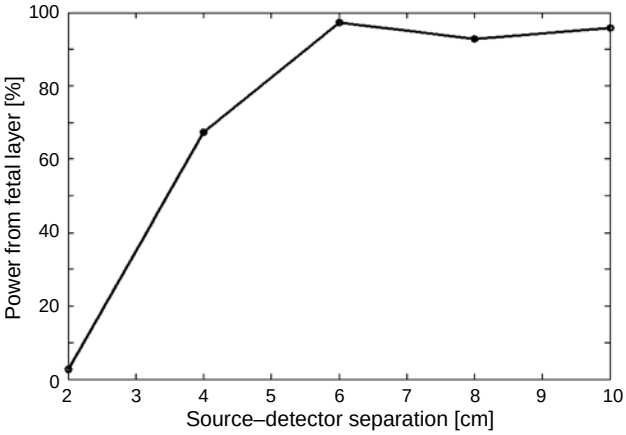

Fig. 6. Percentage power at the fetal layer and the source–detector separation.

fetal signal at this limit. By using the following equation, the expected fetal optical power P_F at –34.7 dB is estimated

$$10\log\left(\frac{P_F}{P_{M+am}}\right) = -34.7 \text{ dB}$$

where P_F is the estimated fetal optical power, P_{M+am} is the optical power at detector (case *i*) in Monte Carlo simulation as mentioned in Section 2.4 and –34.7 dB is the limit of the ANC operation.

As Figure 7 shows, when S–D separation is larger than 4 cm (6 cm, 8 cm and 10 cm), the expected optical power is below photodetector's noise. At a 2 cm and 4 cm source-to-detector separation, the expected fetal optical powers, 2293.99×10^{-12} W/cm^2 and 5.94×10^{-12} W/cm^2, respectively, are higher than the photodetector's noise

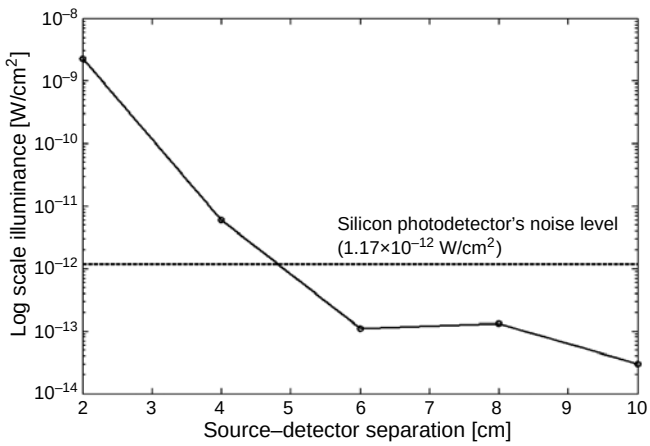

Fig. 7. Estimated P_F (–34.7 dB) at a 2.5 cm fetal depth.

T a b l e 3. Differences in the hardware configuration used in previous studies.

Author	Emitter	Detector	Source–detector [cm]
RAMANUJAM *et al.* [4]	Halogen lamps (4×20 W) and tungsten lamp (2×0.575 W)	A pair of photodiodes	7
CHOE *et al.* [5]	Three laser diodes with a total power of 15 mW	Avalanche photodiode	4–10
CHANCE [7]	Nine laser diodes	Four photomultipliers	10
VINTZILEOS *et al.* [8]	Light-emitting diodes (735, 805, and 850 nm)	Photomultiplier	7–11
OFHR system	IR LED	Silicon detector	4

(1.17×10^{-12} W/cm^2) level. The photodetector is assumed to be operated at the photovoltaic condition with 1000 Hz bandwidth and 1 cm^2 active area. Therefore, the source--to-detector separation of 4 cm, which results in 70% of optical power from fetal layer, is suitable to use with this low noise photodetector. At a 890 nm and 4 cm source–detector separation, the sensitivity of receiver is optimized by considering the limitation of the adaptive filter in FHR detection.

3.4. Comparative study

Table 3 shows a comparison between the optical fetal heart rate (OFHR) system and systems proposed by other researchers. The OFHR system is low power, low cost (the use of expensive and bulky photomultiplier tube is eliminated), wearable and utilizes a robust adaptive filtering to enhance the acquired signal compared to other systems proposed.

4. Conclusions

The Monte Carlo simulations using the three-layer tissue model showed that the expected optical power output is in the range of 10^{-6}–10^{-10} W/cm^2 (1 mW input power) depending on the S–D separation. The use of silicon photodetector and adaptive filtering has limited the S–D separation to 4 cm. At 4 cm S–D separation, 70% of the detected optical power comes from the fetal layer. This is a practical compromise between signal level and percentage of light as indicated by Monte Carlo simulation.

This technique can be applied to detect the FHR and fetal oxygen saturation non-invasively via maternal abdomen in the late gestation week. As indicated in the simulation results, the signal at more than 2.5 cm fetal depth has low SNR. This becomes the first limitation of the optical technique.

Currently, the optical fetal heart rate detection system has been designed and developed in Universiti Kebangsaan Malaysia (UKM). The probe will be enhanced

with an array of LEDs to automate the selection of position with high SNR ratio. A phantom mimic to the human tissue will be designed and developed to test the performance of the system developed before the clinical data acquisition.

Acknowledgements – The authors would like to thank Universiti Kebangsaan Malaysia for sponsoring this work under the Research University Grant: UKM-AP-TKP-07-2009.

References

[1] SINICHKIN Y.P., KOLLIAS N., ZONIOS G.I., UTZ S.R., TUCHIN V.V., *Reflectance and fluorescence spectroscopy of human skin in vivo*, [In] *Handbook of Optical Biomedical Diagnostics*, Vol. PM107, SPIE Press, Washington, 2002, pp. 727–785

[2] BOAS D.A., BROOKS D.H., MILLER E.L., DIMARZIO C.A., KILMER M., GAUDETTE R.J., ZHANG Q., *Imaging the body with diffuse optical tomography*, IEEE Signal Processing Magazine **18**(6), 2001, pp. 57–75.

[3] VO-DINH T., *Biomedical Photonics Handbook*, CRC Press, Florida, 2003.

[4] RAMANUJAM N., VISHNOI G., HIELSCHER A.H., RODE M.E., FOROUZAN I., CHANCE B., *Photon migration through the fetal head in utero using continuous wave, near infrared spectroscopy: Clinical and experimental model studies*, Journal of Biomedical Optics **5**(2), 2000, p. 173.

[5] CHOE R., DURDURAN T., YU G., NIJLAND M.J.M., CHANCE B., YODH A.G., RAMANUJAM N., *Transabdominal near infrared oximetry of hypoxic stress in fetal sheep brain in utero*, Proceedings of the National Academy of Sciences **100**(22), 2003, pp. 12950–12954.

[6] NIOKA S., IZZETOGLU M., MAWN T., NIJLAND M.J., BOAS D., CHANCE B., *Fetal transabdominal pulse oximeter studies using a hypoxic sheep model*, The Journal of Maternal-Fetal and Neonatal Medicine **17**(6), 2005, pp. 393–399.

[7] CHANCE B., *Transabdominal Examination Monitoring and Imaging of Tissue*, U.S. Patent 2005/0038344A1, 2005.

[8] VINTZILEOS A.M., NIOKA S., LAKE M., PENGCHENG LI, QINGMING LUO, CHANCE B., *Transabdominal fetal pulse oximetry using near-infrared spectroscopy*, American Journal of Obstetric and Gynaecology **192**(1), 2005, pp. 129–133.

[9] ZOURABIAN A., SIEGEL A., CHANCE B., RAMANUJAM N., RODE M., BOAS D.A., *Trans-abdominal monitoring of fetal arterial blood oxygenation using pulse oximetry*, Journal of Biomedical Optics **5**(4), 2000, pp. 391–405.

[10] ZAHEDI E., BENG G.K., *Applicability of adaptive noise cancellation to fetal heart rate detection using photoplesthysmography*, Computers in Biology and Medicine **38**(1), 2008, pp. 31–41.

[11] GAN K.B., ZAHEDI E., ALI M.A.M., *Trans-abdominal fetal heart rate detection using NIR photopleythysmography: Instrumentation and clinical results*, IEEE Transactions on Biomedical Engineering **56**(8), 2009, pp. 2075–2082.

[12] WANG L., JACQUES S.L., ZHENG L., *MCML – Monte Carlo modeling of light transport in multi-layered tissues*, Computer Methods and Programs in Biomedicine **47**(2), 1995, pp. 131–46.

[13] Lambda Research Corporation, *TracePro Software for Opto-Mechanical Modeling: The Closest Thing to Working at the Speed of Light*, http://www.lambdares.com/products/tracepro/index.phtml, (accessed November 10, 2005).

[14] BRONZINO J.D., *The Biomedical Engineering Handbook*, Vol. 1, CRC Press LLC, Florida, 2000.

[15] LOUNSBURY K.L., *Anatomical Model*, U.S. Patent 5104328, 1992.

[16] JACQUES S.L., RAMANUJAM N., VISHNOI G., CHOE R., CHANCE B., *Modeling photon transport in transabdominal fetal oximetry*, Journal of Biomedical Optics **5**(3), 2000, pp. 277–282.

[17] REUSS J.L., *Arterial pulsatility and the modeling of reflectance pulse oximetry*, Proceedings of the 25th Annual International Conference of the IEEE EMBS, Cancun, Mexico, 2003, pp. 2791–2794.

[18] RICHARDS D.S., ALLEN S.G., WHITE M.A., PEREZ D.R., *Umbilical vessels: Visualization*, Department of Obstetrics and Gynecology, University of Florida College of Medicine, 1992, http://www.thefetus.net, (accessed September 12, 2005).

[19] MANNHEIMER P.D., CASCIANI J.R., FEIN M.E., NIERLICH S.L., *Wavelength selection for low-saturation pulse oximetry*, IEEE Transactions on Biomedical Engineering **44**(3), 1997, pp. 148–158.

Received April 26, 2011